최근 자기공명 의료영상기기의 발전

조장희[01], 노용만[1,2], 정순철[1], 박세혁[1], 문치웅[3]
1. 한국과학기술원 정보및 통신공학과
2. 대전대학교 전산과 3. 아산생명과학연구소

Recent Developments in Magnetic Resonance Imaging

Z.H. Cho[01], Y.M. Ro[1,2], S.C. Chung[1], S.H. Park[1], C.W. Mun[3]
1. Dept. of Information & Communication Engineering, KAIST, P.O. Box 201 Cheongyang 2. Dept. of Computer Science, Taejon University, 96-3 Yong woon-dong, Taejon, 3 Asan Institute for life Sciences

ABSTRACT

In last few decades, medical imaging techniques have been developed startling progress. Especially in MRI (Magnetic Resonance Imaging), many imaging techniques such as chemical shift imaging, flow imaging, diffusion and perfusion imaging, fast imaging, susceptibility imaging and functional imaging have been studied and many of them were well known as useful diagnostic instruments. In this paper, recently developing techniques, i.e., NMR microscopy, fringe field imaging and functional imaging will be presented.

1. Microscopy

The prolonged read-out gradient in the conventional imaging usually introduces a number of undesirable artifacts such as chemical shift and susceptibility artifacts. An application of extremely short read-out gradient would be a point or single frequency mapping in K-space. This method has many advantages: such as the susceptibility, chemical shift, and diffusion effects free images can be obtained (1). The KPM method is ideally suited for microscopy, where gradient coils are usually small and, therefore, it is easy to obtain a fast and strong gradient (2).

K-space Point Mapping (KPM) Technique.

For the sake of simplicity, let us assume that we have a one-dimensional case of NMR imaging with an object space density function $\rho(x)$, the signal obtained would be,

$$S(t_x) = \int_{-\infty}^{\infty} \rho(x) e^{-ix\gamma\int_0^{t_x} G_x(t')dt'} dx. \quad [1]$$

A complete data set, then, will represent the frequency spectrum of the object from dc to a maximum frequency of $\gamma G_x t_x/2\pi$, where t_x is the read-out gradient time duration. If time is discrete, i.e. $t_x = n\Delta T_x$, Eq. [1] can be written as

$$S(n\Delta T_x) = \int_{-\infty}^{\infty} \rho(x) e^{-ix\gamma G_x n\Delta T_x} dx. \quad [2]$$

Equation [2] represents a specific frequency component corresponding to a time $n\Delta T_x$ for a given constant strength gradient G_x. Therefore, Eq. [2] can also be written as a function of $K_x(t)$ which is given by

$$K_x(t) = K_x(n\Delta T_x)_{\Delta G_x} = \gamma\int_0^{t_x} G_x(t')dt' = \gamma\int_0^{n\Delta T_x} \Delta G_x dt' = \gamma\Delta G_x n\Delta T_x. \quad [3]$$

In Eq. [3], $G_x(t')$ is assumed as ΔG_x. Conversely, one can also write Eq. [3] as

$$K_x(g_x) = K_x(n\Delta G_x)_{\Delta T_x} = \gamma\int_0^{g_x} \Delta T_x dg_x' = \gamma\int_0^{n\Delta G_x} \Delta T_x dg_x' = \gamma\Delta T_x n\Delta G_x. \quad [4]$$

The basic difference between Eq. [3] and Eq. [4], however, is that Eq. [3] is continuous in time within a given T_R while Eq. [4] is not, since time is fixed to a short period ΔT_x with $n\Delta G_x$ as a variable for a given T_R. Therefore, Eq. [4] represents only one frequency component at a given sequence, that is it represents only one point in K_x. Equation [3] is simply a line scan technique, while Eq. [4] is a point scan method in K-space. Naturally, extension of the method to 3-D volume imaging is obvious, and each encoding in this case represents a frequency point in 3-D K-space and a general 3-D equation would simply be given as

$$S(g_x, g_y, g_z) = \int_{-\infty}^{\infty}\int\int \rho(x,y,z) e^{-i(x\gamma n\Delta G_x\Delta T_x + y\gamma n\Delta G_y\Delta T_y + z\gamma n\Delta G_z\Delta T_z)} dxdydz, \quad [5]$$

where g_x, g_y, g_z are the x,y,z gradients of variable amplitudes with a fixed pulse width ΔT_x, ΔT_y, and ΔT_z, respectively.

Advantages of the method are many, including short echo time (T_E), which leads to reduction of susceptibility, chemical shift, and diffusion effects. Because of the short echo time, the method also improves the SNR (Signal to noise ratio) since the signal obtained does not suffer T_2-decay. In addition, the narrow bandwidth (single frequency) of the detected signal will also improve the signal to noise ratio. The disadvantage of the method, however, is long data acquisition time, in spite of possible reduction of T_R to as short as 1 ~ 2 msec.

Extended KPM Technique--Multiple KPM (MKPM) technique for data acquisition time improvement

As mentioned above, an extremely small echo time allows us to detect a single frequency in K-space, and consequently susceptibility and chemical shift effects can be reduced drastically through reduction of the echo time. However, this extremely short echo time (ΔT = 10 ~50 μsec) is not a strict requirement for most

imaging situations, even where strong magnetic fields are essential to ensure required high resolution, such as NMR microscopic applications. Therefore, ΔT can be enlarged substantially, by a factor of five or ten, without great risk of increasing the susceptibility or chemical shift effect; that is, one can improve the scanning time by simply extending the single point scan (in K-space) to a five or ten point scan. It will then easily lead to a proportionally improved data acquisition time without loss of the advantages gained by the original single point KPM technique. An example of the extended MKPM method is illustrated in Fig.1, where 5 point (n=5) scanning is given as an example. By employing the MKPM method, an excessively large scanning time can be avoided without great risk of increasing the inhomogeneity effects.

Simulation Results

A computer simulation study was performed to estimate the degree of susceptibility artifacts in the image and the time required for the image data acquisition for the MKPM technique when applied to NMR microscopy. A 2-D phantom (radius of 50 μm) was used which consists of an air cylinder (radius of 10 μm) surrounded by water which has a different susceptibility. Using the field inhomogeneity obtained, K-space data of conventional frequency encoding technique and MKPM technique were calculated. For the examination of the extended MKPM technique, a five point MKPM experiment was performed and data was acquired, i.e., n=5 was used with ΔT=20μsec. After calculating K-space data for each technique, images were reconstructed. Figure 2 shows the comparison of the simulated images obtained by the conventional frequency encoding technique and the MKPM technique. As shown, Fig. 2(b) shows severe susceptibility artifacts as well as resolution degradation. However, by using the MKPM technique, the susceptibility artifacts are reduced, and resolution degradation is more or less eliminated as shown in Fig 2(c). Figure 2(a) is the original image given as a reference.

In conclusions, the extended multipoint K-space point mapping (MKPM) technique preserves the inherent advantages of the original KPM method yet having a potential of improving data acquisition time. This is applicable in many areas of micro NMR imaging where diffusion and inhomogeneity effects such as susceptibility effects are of the prime concern.

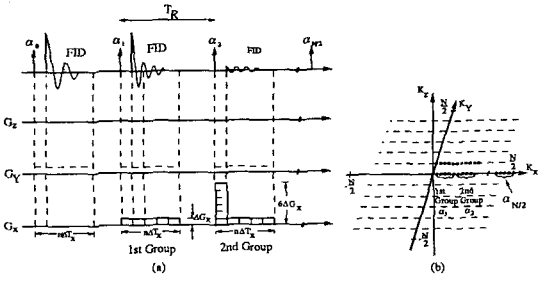

Figure 1. (a) Extended Multiple K-space point mapping technique (MKPM) which extends the ΔT by a multiple of n. (b) K-space correspondence of the pulse sequence given in (a).

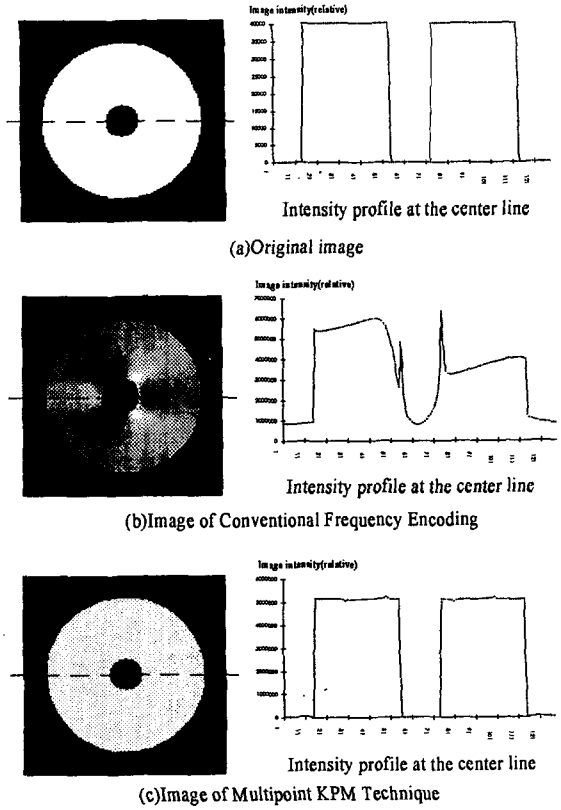

Figure 2. Simulated phantom images of (a) ideal case (the original image), (b) the susceptibility distorted phantom image obtained by the conventional frequency encoding, and (c) the image obtained by the 5 point MKPM technique.

2. Fringe Field

Nowadays, many investigators are interest in inexpensive high field magnet for more advanced MR study, such as brain functional imaging and spectroscopy. And another requirement is the compatibility for claustrophobia patients. MR fringe field imaging modalities with single and two magnets will be suitable for above requirements. This will introduce the economical high field MR system (more than 4T) which can be installed in small room space and will be comfortable for claustrophobia patient in the case of two magnet system. In addition, the open space of fringe field MRI with two magnet may be helpful to perform surgery and MRI simultaneously.

The most severe problem of fringe field imaging is field inhomogeneity, built-in gradient. This inhomogeneity is too large to be controlled by using externally added gradients, when the imaging regions moved away from the central region. Strong built-in gradient used for slice selection requires high rf power for reasonable slice thickness. The selected slice plane in transaction image has curved shape and thickness is spatially variant depends on the magnet field profile. The motion artifact under the strong built-in gradient is severe. Finally, the stronger built-in gradient causes the more loss of signal due to diffusion effect.

Method

We considered three approaches to generate fringe field images with commercially available magnet. The first method is the use for the fringe field inside magnet with a suitable bore size (scheme I, in Fig.3). In the case of human brain, the magnet bore size must be reasonably large so that the human head can be placed inside the bore with all the necessary gradients and rf coils. Imaging algorithms would require either inhomogeneity correction or imaging of the curved planes with FM modulated rf pulses to cover wide frequency band under the strong z directional built-in gradient. The second method is the use for the fringe field outside the bore of single small bore magnet (scheme II, in Fig.3). The third method is to use two magnets with small bore magnets to form a combined fringe field which would allow us to image the human brain or any localized part of the human body (scheme I, in Fig.3).

Computer Simulation

Some preliminary study has been performed by computer simulation. Magnet field mappings for each scheme were simulated by assuming that 2.0 T magnet had four active-wire loop positioned at ±20 and ±50 cm from magnet center (that is, 1m of length) with same diameter (100 cm). We assumed that the current distribution for each loop same. Built-in gradients in z-direction were calculated from the above field mappings.

In scheme I and II, image planes obtained will be distorted and parabolically curved following the gradient pattern in x, y, and z direction. This phenomenon was also simulated using specially designed phantom. Inside of rectangular phantom, there five cones of which apexes are facing the outside of magnet (in z direction) and placed in parallel. Assuming the phantom locates apart from the center of magnet (25 cm, and 150 cm) but at the diagonal center, the effects on image due to curved shapes of selected slice were also simulated.

A 3D pulse sequence based on spin echo technique was used for correcting the effects of inhomogeneity created by the various fringe fields. Built-in gradient in z direction was used as both slice selection and readout gradient. G_x and G_y were used as phase encoding gradients. A wide bandwidth of rf pulse required to select a plane or a volume with a reasonable slice thickness under a strong built-in gradient. One way to distribute the confined rf signal in time domain is to use a FM pulse on a linear sweep. We know quadratic phase problem when one uses FM rf pulse rather than AM pulse can be circumvented by the FM curved chunk 3-D sequence. Since the phase is relatively constant within a plane, each plane can be reconstructed without much loss of signal in the chunk 3D imaging, or later 2-D image may be reconstructed by the superposition of the 3-D images along the z direction after taken magnitude.

Results

Available imaging region is restricted to 0~20 G/cm of built-in gradient associated with signal loss due to diffusion effect and band limit of rf system. As expected, built-in gradient of scheme III(in Fig.4) was much less significant among three method. Simulation results of scheme II(in Fig.3), however, is not practical because built-in gradient near magnet edge is too strong but magnetic field at far away where small built-in gradient become too weak. The shape of selected shape was shown as parabolically curved plane by simulation. And an experimentally obtained images support the feasibility of MR fringe field imaging modality. To extend the imaging region further study being performed including the special design of magnet and shimming coil for fringe magnet. Even though this study uses commercially available magnet, this shows the feasibility of fringe field imaging to provide economic and comfortable high field MRI system (3-6).

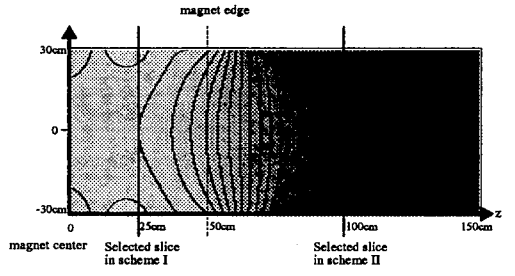

Figure 3. Magnetic Field Contour (1015 G/Contour) in single bore.

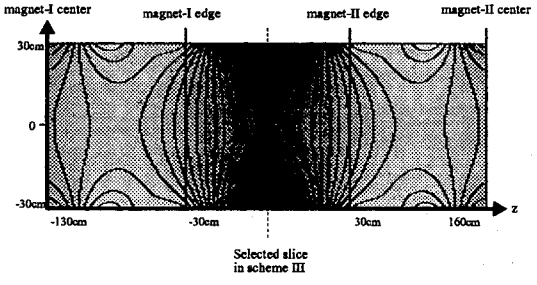

Figure 4. Magnetic Field Contour (387 G/Contour) in double bore.

3. Functional Imaging

A. Analysis of Inflow and Susceptibility Effects

Current MR functional imaging is believed to be based on T2* effect by using gradient echo imaging technique with a relative long echo time (TE) and short repetition time (TR), and relatively large flip angle (α)(7). These fast gradient echo techniques are, however, not only sensitive to T2* effect but also extremely sensitive to the inflow effect from unsaturated venous blood flowing into the imaging slice. Therefore, the conventional gradient echo technique(CGE) appears to be generating the signal which is a mixture of inflow effect and susceptibility effect. In this topic, it has been shown that the signal change is affected by flip angle α, echo time TE, repetition time TR and both inflow effect and susceptibility effect are strongly affected by above three parameters. Although we have obtained susceptibility affected-signal change by CGE technique with small flip angle and long echo time, the results so far obtained are relatively poor signal to noise ratio and appear to be contaminated by large fraction of inflow effect. In this topic, we report some of the results which we have systematically analyzed by varying flip angle (α), repetition time (TR), and echo time (TE). Experimental results obtained with 2.0T MR scanner indicate that the observation of the pure susceptibility effect is limited by the inflow effect or poor signal to noise ratio.

Theory

Recently, the steady-state free precession(SSFP) or gradient echo imaging techniques has been widely used for the time course study in functional MR imaging(fMRI). In this case the transverse magnetization M which generate echo signal by SSFP technique is given by

$$M = M_0 \frac{1-\exp(-TR/T1)}{1-\cos(\alpha)\exp(-TR/T1)} \sin(\alpha)\exp(-TE/T2) \qquad [6]$$

Equation [6] indicates that if the repetition time is shorter than the T1 relaxation time, resultant magnetization would be small. In other words, static spin signal is suppressed, but if flowing spin exists, i.e., the unsaturated flowing spins entering into the selected slice signal will be generated unlike the static tissues. This appears the basic inflow signal enhancement mechanism. This inflow effect in gradient echo, however, is affected by several factors such as the flip angle α, echo time TE and repetition time TR. It is, therefore, strongly suspected that the flow effect plays an important role in gradient echo functional imaging where TR and TE are usually short while α is kept relatively large. Although, the inflow effect is an important indicator of the physiological and functional behaviors in relation to the external sensory stimulations, it is believed to be of no direct relation to the oxygen level or susceptibility effect. It is an independent factor likely to be observed when the imaging slice or selected region contains large veins, for example relatively large veins near the visual cortex in case of visual stimulation. If, therefore, pure oxygen level or deoxyhemoglobin level measurement is the prime importance, inflow effect would appear as a nuisance and if possible should either be eliminated or at least measurable so that desired correction can be made.

Experiments

A series of conventional gradient echo(CGE) experiments by varying α, TE, and TR were performed on a 2.0 Tesla whole body system with a surface coil. Functional imaging by photic stimulation was carried out by using CGE technique. For the time course studies, flip angles of 30° to 90°, repetition times of 35 to 65ms, and echo time of 16 to 35ms were used. Imaging time of 7sec was used for single slice of 8mm thick which was located at the occipital pole near the calcarine fissure. In each experiment, 50 continuous image sets were collected and used for time course study and all the stimulation was applied uniformly from image number 11 to 20 by the visual stimulator.

Figure 5 shows the time course data of the signal change by varying repetition time TR from 35ms to 65ms in three steps for flip angles of 90°, 50°, and 30°, respectively. For this experiment, to examine the inflow effect, a relatively short echo time TE=16ms was used. As shown in Fig.5, the inflow effect is pronounced as flip angle increases. Similar trend is also observed as the repetition time decreases. If, indeed, inflow effect is dominant factor, these observations are expected. On the other hand increasing susceptibility effect should be observable as flip angle decreases with increasing repetition time as well as echo time. The signal change observed at small α with a relatively large TR which believed to be of the susceptibility effect dominant, however, appears small and signal to noise ratio is poor. Fig.5 is a clear indication of the strong and dominant role of inflow effect observed in many fMRI. Fig.6 another time course study data obtained with varying echo time TE are shown, namely TE of 16ms, 25ms, and 35ms, respectively with varying flip angle α of 90°, 50°, and 30°. In this case, in an attempt to observe the susceptibility effect, a relatively large repetition time is used, i.e., TR=55ms. As is shown, still pronounced inflow effect is seen with small TE(=16ms). By increasing the echo time, however susceptibility effect begun to show and effect of flip angle is no longer pronounced as in the case of short TE(=16ms). The signal change at large TE(=35ms) is still suspected for some inflow effects, but the signal change observed could be largely by susceptibility effect. As evidenced from the data, overall signal decay is clearly visible as TE increases but remains relatively constant, suggesting that the susceptibility contrast is not as strongly affected as the inflow signal. In Fig.7, another view of the experimental data shown in Fig.5 is displayed. This also clearly shows the significant inflow effect.

Thus, using the conventional gradient echo technique one can observe the signal change that is affected by two factors, i.e., inflow and susceptibility effects. Since the obtained signal intensity or signal to noise ratio is inversely proportional to the TE while the susceptibility contrast is linearly proportional to the TE, it is difficult to increase both the susceptibility contrast as well as signal

to noise ratio. Present study confirms that with the conventional gradient echo technique there is substantial amount of inflow effect, therefore, it appears difficult to observe purely quantitative oxygen metabolisms in brain function study unless another new pulse schemes are derived, such as the tailored RF pulse technique to be presented(8).

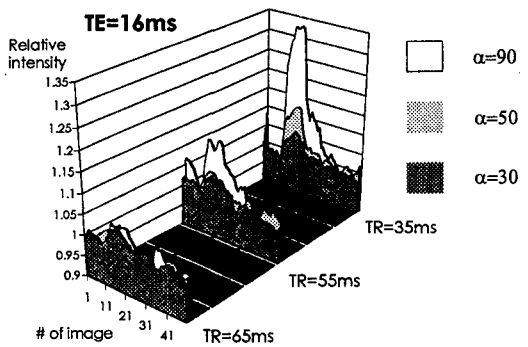

Figure 5. Time course of signal change observed by CGE technique in small vein near the visual cortex with varying TR(35ms, 55ms, 65ms) and α (90°,50°,30°) while TE(=16ms) is fixed. z-axis is signal intensity, while y-axis and x-axis are TR and image number, respectively.

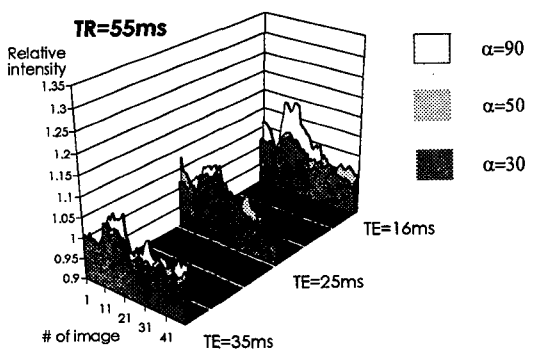

Figure 6. Same as Fig.5 with varying TE(16ms,25ms,35ms) and α (90°,50°,30°) while TR(=55ms) is fixed. z-axis is signal intensity, while y-axis and x-axis are TE and image number, respectively.

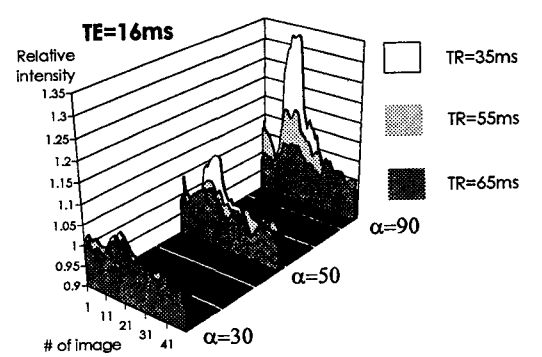

Figure 7. Same as Fig.5 with varying α (90°,50°,30°) and TR(35ms,55ms,65ms) while TE(=16ms) is fixed. z-axis is signal intensity, while y-axis and x-axis are α and image number, respectively.

B.NMR Functional Imaging-A True Susceptibility Measurement Technique

The sensitivity of a gradient echo NMR to the susceptibility or the local magnetic field gradient provides a means to detect differences in tissue oxygenations that are due to the amounts of the paramagnetic deoxyhemoglobin produced in the capillary. Recently, the effects have been exploited to study human brain functions by gradient echo imaging techniques, which is particularly sensitive to the local magnetic susceptibility(8,9). The conventional gradient echo imaging technique which is believed to be sensitive to the T_2^* effect due to the local susceptibility, however, also sensitive to the in-flow effect of arterial as well as venous blood, thereby, complicates the analysis of the functional image data. The signal changes believed to be dependent on the susceptibility during the external stimulation, i.e., the time course signal intensity variation is dependent on the several factors such as RF pulse flip angle α, echo time TE, repetition time TR, and is not only sensitive to T_2^* effect but also extremely sensitive to the in-flow effect from the fresh unsaturated spins entering into the imaging slice(7).

Some of those problems can be overcome by using a new pulse sequence known as tailored radio frequency gradient echo(TRFGE) technique which will be introduced in the following(10). This proposed TRFGE technique has been used for the venography, and uses the tailored RF pulse which enhances the signal intensity especially when the susceptibility effect exists but suppresses otherwise. As will be reported, using TRFGE technique we have obtained functional imaging mainly due to the susceptibility, not mixed with in-flow effect. The latter is an unique advantage of the TRFGE method compared with the other gradient techniques most of which suffer large in-flow effect thereby complicates the true oxygenation measurement.

Theory

Let us assume that the selected slice thickness (z) is larger than the transverse directional resolution(x,y), thus, the susceptibility in a voxel, is more or less sensitive to the z-directional inhomogeneity when the gradient echo technique is used for imaging. In an ideal case with no field inhomogeneity, by application of a rectangular slice selection RF pulse(sinc pulse), all the spins in the slice will be well-refocused, therefore, result in a large signal. If field inhomogeneity due to the magnetic susceptibility is introduced, i.e., a strong localized gradient exists within a voxel in z direction, then the phase distribution will be incoherent, and the resulting signal which is the vector sum of all the spins will be a weak signal (10).

If the local susceptibility or susceptibility gradient exists, it usually exhibits strong localized field gradient thereby dephases all the spins within the voxel and makes signal sum to nearly zero(9). If a slice selection RF is designed so that it has a bi-linear phase distribution around the slice center along the slice selection direction, it is possible to refocus the dephased spins due to the local susceptibility. On the other hand, in normal tissue, where no

susceptibility exists, the phase of the spin will be dephased therefore spin phase will be incoherent. In another word, the latter case, the phase distribution generated will be solely by the RF, therefore, the resultant phase distribution will be bi-linear or totally dephased. Let us first consider the case of the local susceptibility imaging. In this case, the phase distribution will become partially coherent when the tailored RF pulse is applied. According to the relation given by

$$S = \left| 2\pi M z_0 \, \mathrm{sinc}\left(\frac{P_{sus}}{2\pi} z_0\right) * \mathcal{F}^{-1}\left[\exp\left(i\frac{4\pi}{z_0}|z|\right)\right] \right| \qquad [7]$$

where M and P_{sus} are the magnetization and susceptibility phase gradient, respectively, and * represents the convolution operator. The unique feature of this result is that, on the contrary to the case of normal tissues, the signal intensity will increase linearly with increasing phase gradient value, i.e., signal intensity will increase with the increase of the local susceptibility. Using this fact, susceptibility effect enhanced imaging using TRFGE technique can be accomplished.

On the contrary, in the conventional gradient echo(CGE) imaging, the signal change is not only affected by the susceptibility but also affected by the in-flow effect of the blood flow of both arterial and venous blood. In CGE, according to the RF flip angle α , TE, and TR, the signal intensity due to both susceptibility and in-flow effect will vary. For example, the susceptibility contrast increases with the increase of echo time, but the signal loss also increases thereby decreases overall SNR. As has been reported in the separate report to be presented in this meeting, this apparent controversy can be overcome by use of the TRFGE.

Experiments

With a 2.0T whole body MRI with a surface coil, a series of experiments using the TRFGE imaging sequence were carried out and compared with the conventional gradient echo(CGE) technique. For the time course study, TR of 35 to 65ms, TE of 16 to 35ms, and, RF flip angle of 30° to 90° were used in combination to observe the in-flow effect as well as susceptibility effect. In all experiment, 50 continuous axial image sets near the visual cortex were obtained with the photic stimulation applied in imaging from image number 11 to 20, and rest of the images were obtained without stimulation. Visual activation was applied by photic stimulation using 8Hz LED checker board. Imaging time for single 8mm thick slice was about 7 sec.

The time course data shown in Fig. 8 were obtained by the TRFGE sequence with varying the RF flip angle α from 30° to 90° while TR(=35ms) and TE(=16ms) were fixed. As shown in Fig. 8, nearly identical signal variation, independent of the RF flip angle α, suggests that the signal variation are not affected by the in-flow effect and probably due to the susceptibility effect only. In Fig. 9 another time course data which were obtained by varying the echo time TE from 16ms to 35ms with a fixed TR(=55ms) and RF flip angle(=30°) also suggests that the susceptibility contrast in TRFGE technique is independent of the TE. This latter result is a clearly distinguishable from the conventional gradient echo sequence where decrease of the signal is observed with the increase of TE. In short, TRFGE technique is not sensitive to the in-flow effect and also susceptibility contrast is developed by the RF pulse rather than TE, therefore, is independent of TE adjustment. The latter suggests the use of the short echo time thereby one can eliminate the potential T_2 signal decay.

In conclusion, it has been shown that a tailored RF pulse of suitable form can effectively be used for the measurement of the susceptibility contrast and same time, suppresses the signals from normal tissues. As it has been demonstrated, TRFGE technique is not only more sensitive to the susceptibility contrast but also insensitive to the other effects such as the in-flow effect. TRFGE technique, therefore, probably could be used for the susceptibility only functional imaging, that is the true measurement of the oxygenation and deoxyhemoglobins without the interference from the in-flow effect.

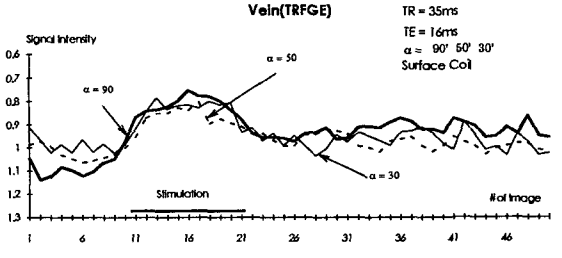

Figure 8. Time course of signal change in a small vein near visual cortex by TRFGE technique with varying α (90°,50°,30°) while TR(=35ms) and TE(=16ms) are fixed.

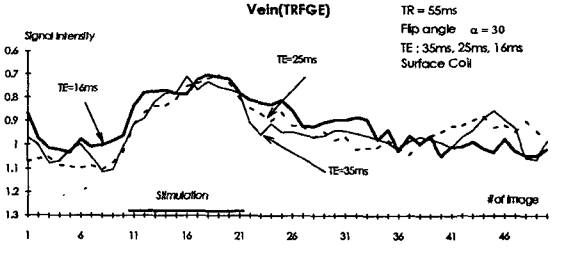

Figure 9. Same as Fig.8 with varying TE(16ms,25ms,35ms) while TR(=55ms) and α (=30°) are fixed.

REFERENCES

1. A. Nauerth, B.Gewiese, and G. Rohr, Brochure published by Bruker, Medizintechnik GmbH (1993).

2. Z.H. Cho, C. B. Ahn, S. C. Juh, H. K. Lee, R. E. Jacobs, S. Y. Lee, J. H. Yi, and J. M. Jo, Med. Phys. 15(6), 815 (1988).

3. H. Darfuss, H. fisher, R. Graumann, D. Hentschol and Ladebeck, "Whole-body MR Imaging at 4.0 Tesla," Book of abstracts in seventh annual meeting of SMRM p.21 (1988).

4. S.Y. Lee and Z.H. Cho,"Localized Volume Selection Technique Using an Additional Radial Gradient Coil," Mag. Reson. Med. Vol.12, 56-63 (1989).

5. Z.H. Cho, D.J. Kim, Y.K. Kim, "Total inhomogeneity correction including chemical shifts and susceptibility by view angle tilting," Med. Phys. Vol.15, 7 (1988).

6. D. Kunz, "Use of frequency-modulated radio frequency pulses in MR imaging experiments," Magn. Reson. Med. Vol.3,377 (1986).

7. R.Turner et al, Magn. Reson. Med. 29, 277-279 (1993).

8. Z.H. Cho, Y.M. Ro, and T.H. Lim, Magn. Reson. Med.28, 25-38 (1992).

9. Y.M.Ro, and Z.H.Cho, Magn. Reson. Med. 28, 237 (1992)

10. J. Frahm et al, Magn. Reson. 29, 139 (1993).